

Synthesis, characterization and electrochemical studies of Polyaniline/Benzalazine/cobalt(II) chloride composite

B. Divya¹, D. Kanagavel², N. Chandralekha² and C. Vedhi^{3*}

¹Department of Chemistry, St. Mary's College (Autonomous), Thoothukudi -628001, Tamil Nadu, India.

²Department of Chemistry, Kamaraj College, Thoothukudi-628003, Tamil Nadu, India.

³Department of Chemistry, V.O.Chidambaram College, Thoothukudi-628008, Tamil Nadu, India.

Affiliated to M.S. University, Tirunelveli - 627 012, Tamil Nadu, India

*Corresponding author: cvedhi23@gmail.com, mobile: 9092368104

Abstract

Composites of polyaniline containing benzalazine and cobalt(II) chloride was synthesized by oxidation polymerization of aniline in the presence of benzalazine and cobalt(II) chloride. UV-Visible and infrared spectral studies were carried out to confirm its formation. X-ray diffraction studies showed its partial crystalline nature. Atomic force microscopy explored its surface morphology. Redox nature was investigated by using cyclic voltammetry. Electrochemical impedance spectroscopy studies were done to study its capacitance behaviour. This composite showed good capacitance at pH 7. Chronocoulometric studies showed that double layer capacitance was more in neutral medium. Charge consumed for electrolysis was found out using bulk electrolysis.

Keywords: polyaniline, benzalazine, specific capacitance.

1. Introduction

Polyaniline is one of the most thoroughly examined polymer. This polymer exhibits very good valuable properties and it can be easily prepared. Its properties like thermal stability, conductance, dielectric

stability etc. can be made better by incorporating some other materials in to its polymer backbone. Such polymer blends is called composites. Enormous literature was available for polyaniline composites. Polyaniline composites with other materials like fly ash [1], metal compounds [2], other polymers [3], egg shell [4], carbon nano tubes [5], clay [6], rice husk [7], etc. had been reported. These polyaniline composites are applied in various fields like adsorption [8], sensing [9], capacitors [10], corrosion inhibition [11], etc.

2. Materials and methods

Aniline was bought from spectrum chemicals and distilled before polymerization. The oxidizing agent potassium perdisulphate was also bought from spectrum chemicals. Cobalt(II) chloride was bought from e-Merck. Ethanol was bought from Jiangsu Huaxi, China. Indium tin oxide (ITO) coated glass plates which were as working electrodes used in cyclic voltammetry and electrochemical impedance spectroscopy studies were provided by e-Merck.

FT-IR spectra was recorded using Nicolet Si5 spectrometer (ATR) (model P-4600). Jasco V-

630 spectrophotometer was used to obtain UV-Visible DRS spectra in the range of 200-900 nm. X'pert PRO power X-ray diffractometer was used to get X-ray diffraction patterns in the 2θ position 10 to 80. The anode material used was copper. Atomic Force Microscopic images were recorded by using Nanosurf easyscan 2 AFM (BT02218) in contact mode. Cyclic voltammograms and electrochemical impedance measurements were done using CH electrochemical work station sinsil CH 650.

3. Experimental

3.1 Synthesis of Polyaniline/Benzalazine/Cobalt(II) chloride composite

Benzalazine was synthesized under microwave irradiation by the reported method [12].

3ml of aniline was magnetically stirred in 100ml of 1M hydrochloric acid for 10 minutes. Then benzalazine and cobalt(II) chloride of 10 weight percentage of aniline was taken and mixed with the above solution and stirred for an hour for dispersion. Then the oxidizing agent potassium perdisulphate was added and stirred for another 4 hours. Then the dark green colored solution obtained was refrigerated for 24 hours. The green precipitate was filtered and dried at room temperature.

4. Results and discussion

4.1 UV-Visible spectral studies

The peak at 309nm is due to the excitation of benzenoid ring in the polyaniline back bone [13]. Because of charge transfer, excitation of quinoid ring takes place and this is seen as a broad peak in the range 490-817nm [14]. π to π^* transition of benzenoid and quinoid and benzenoid rings are present at 255nm. Band for the transition from polaron to π^* is present at 441nm [15].

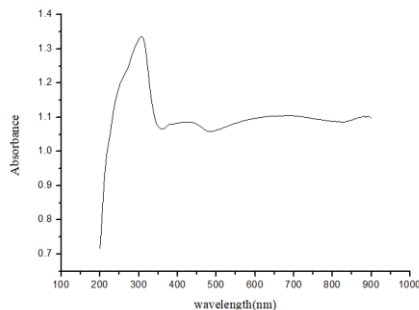


Fig. 1 UV-Visible spectra of the composite

4.2 Infrared spectral studies

The C=C stretch frequency of benzenoid ring is present at 1491cm^{-1} [16,17] and quinoid [17]. The peak at 3447 cm^{-1} is due to N-H stretching [18]. The peak at 1134cm^{-1} is owed to C-H in plane bending of N = Q = N [14]. This peak is associated with the protonated form of polyaniline which is

conductive. Peak for C-H out of plane bending for 1,4-disubstituted polyaniline is found at 879 cm^{-1} [18]. The peak at 1299 cm^{-1} is due to C-N stretching of secondary amine group [19]. The peaks present at 2923cm^{-1} and 2853cm^{-1} are ascribed as aromatic C-H stretch and aliphatic C-H stretch respectively.

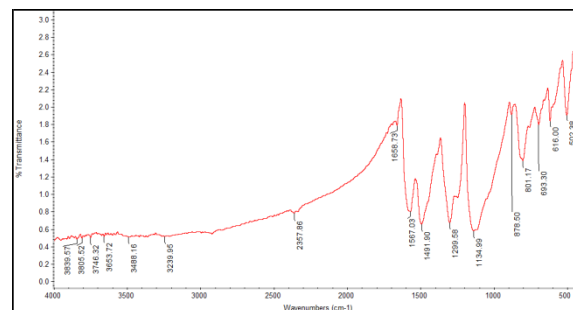


Fig.2 Infrared spectrum of the composite

4.3 X-ray diffraction studies

The peak with maximum intensity is at the 2θ position 25. 24 and this corresponds to 110 plane of polyaniline [20]. The peak at 2θ position 20.18 corresponds to 100 plane of polyaniline [20]. For pure polyaniline crystallinity of 9.64% had been reported by Hichem Zeghoud et.al. [21] Crystallite size is calculated using Scherrer's equation

$$\text{Crystallite size} = 0.94 \lambda / \beta \cos \theta$$

λ – wavelength of x-rays

β = Full width half maxima

θ = Bragg's angle

Crystallite size was found to be 11nm. The percentage of crystallinity of this composite is 16. A very little increase in the crystallinity of the composite is due to the incorporation of benzalazine and cobalt(II) chloride into the polymer matrix.

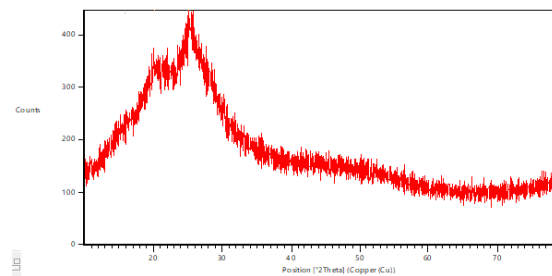


Fig. 3 X-ray diffraction pattern of the composite

4.4 Scanning electron microscopy

Particles are well aggregated and no discrete particles are present in the SEM image. Aggregated structure with flat surface is seen in the SEM image of the composite.

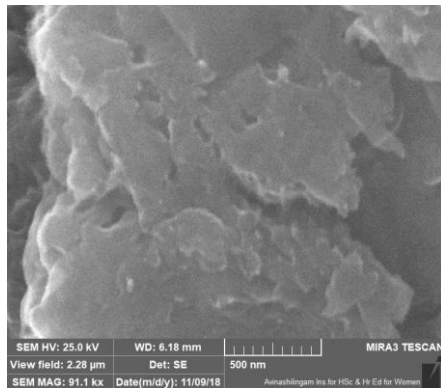


Fig. 4 SEM image of the composite

4.5 Atomic Force microscopy

Flat surface was seen in the topography of the composite. Various shapes and structures had been reported in the literature. Spherical shape [23], flat structure[24], wrinkled structure [25] for polyaniline had been reported in the literature. Aggregated particles with flat surface are seen in the topography of this composite.

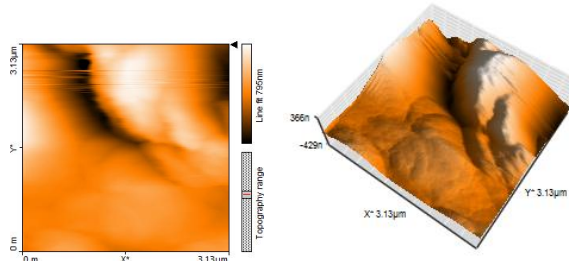


Fig. 5 a)Topography of the composite b)3D view

Table 1 Roughness values for the composite from the topography

Roughness	Average roughness (nm)	Root mean square roughness (nm)
Line (Width 3.125μm)	126.88	142.27
Area (Area 9.842pm ²)	108.80	147.80

4.6 Cyclic Voltammetric studies

Cyclic voltammograms were taken for the composites in pH 1, 7 and 13 by coating the composite on Indium tin oxide substrate. These were used as the working electrode. Reference electrode was Ag/AgCl and platinum electrode was used as

counter electrode. Measurements were made on the scan rates of 25, 50, 75 and 100mV/s.

In this composite at pH 1, one oxidation peak is obtained. This peak is the merged peaks of the oxidation of leucoemeraldine to emeraldine and oxidation of emeraldine to pernigraniline states. Similarly the corresponding merged reduction peak is also obtained in the cyclic voltammogram of the composite [26]. The maximum oxidation potential is at 0.597V and reduction potential is obtained at -0.137V for the scan rate of 100mV/s. Here no peaks of benzalazine are seen in the cyclic voltammograms of this composite.

In pH 7 well defined peaks are not clearly seen on the cyclic voltammogram. Only the reduction peak of benzalazaine is slightly visible. In the composite only the reduction peak of benzalazine is visible at pH 13 also. No peaks are obtained for the oxidation and reduction of polyaniline. The reduction of benzalazine is obtained at -0.995V for the scan rate of 100mV/s [12].

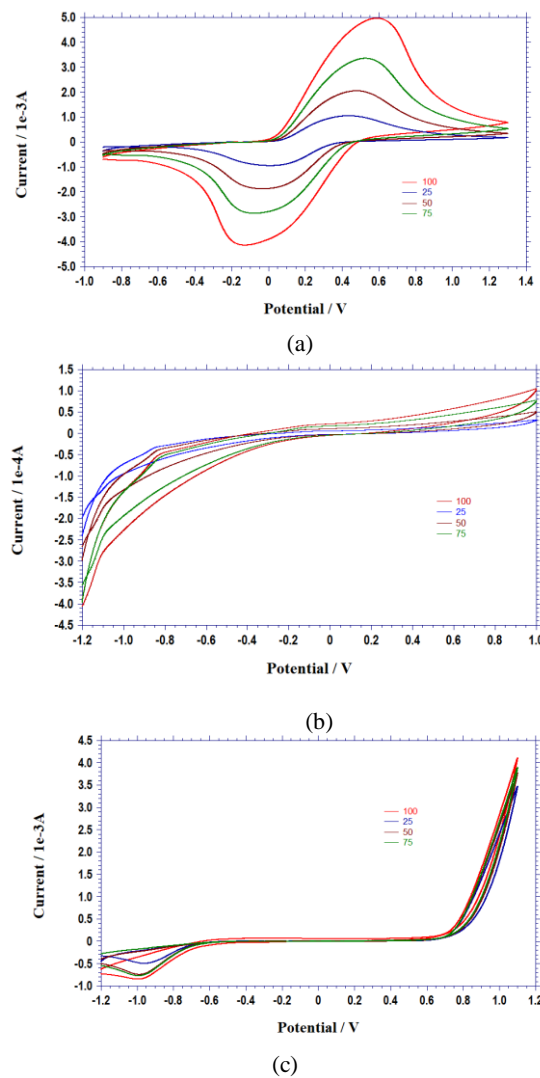


Fig. 6 Cyclic voltammograms of the composite at a)pH 1 b)pH 7 and c)pH 13

4.7 Electrochemical impedance spectroscopy

Electrochemical impedance spectroscopy was done with the same cell set up as in cyclic voltammetry. Measurements were made in pH 1, 7 and pH 13 and the acquired data was fitted by using Randles circuit. A semicircle called Nyquist plot is obtained. From the Nyquist plot resistance and capacitance are noted and tabulated in table 1.

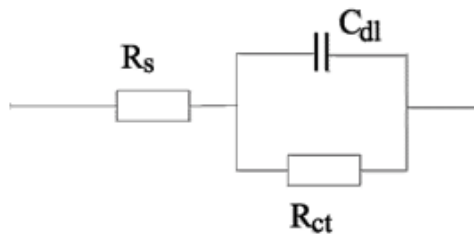
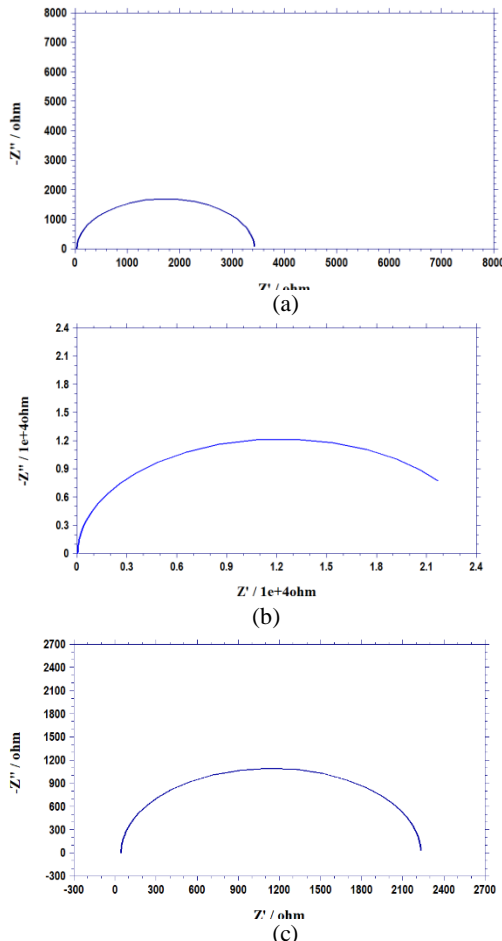


Fig. 7 Randles circuit



**Fig.8 Nyquist plots of the composite at
a)pH 1 b)pH 7 c)pH 13**

Table 2 Resistances and specific capacitance of the composite at pH 1, 7 and 13

pH	Solution resistance (ohm)	Charge transfer resistance (ohm)	Specific capacitance ($\mu\text{F}/\text{cm}^2$)
1	34.73	3396	35.6
7	49.97	2.439e4	78.7
13	45	2188	36.8

From bode plots magnitude of impedance and phase angle can be noted. From the plot solution resistance and double layer capacitance are clearly seen on the Y-axis. The specific capacitance of this composite is $78.7 \mu\text{F}/\text{cm}^2$ at pH 7. This is the maximum specific capacitance for this composite. In acidic and basic media, less specific capacitance is shown by this composite. The maximum phase angle shown by this composite at pH 1 is -73° . At pH 7 it showed a maximum phase angle of -81° and at pH 13 it shows the phase angle of -72° . For capacitors which are ideal the phase angle should be -90° [27].

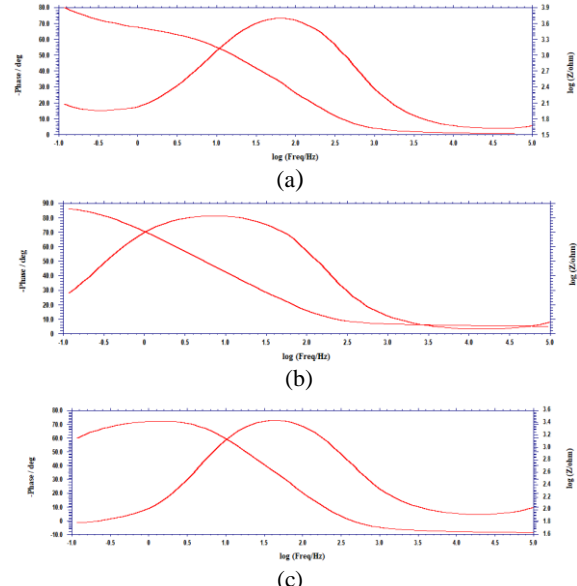


**Fig. 9 Bode plots of the composite at
a)pH 1 b)pH 7 c)pH 13**

4.8 Chronocoulometric studies

Chronocoulogram of the composite shows that charging takes place at a constant speed with the increase of time. The discharging is slow. This shows that reduction reaction of this composite is taking place at a faster rate than oxidation. The intercept in the reduction reaction i.e. the forward step is obtained due to the presence of double layer capacitance [28]. The difference in the intercepts of forward scan and the reverse scan gives the surface charge. [29, 30]. Double layer capacitance and surface charge is more for this composite at pH 7.

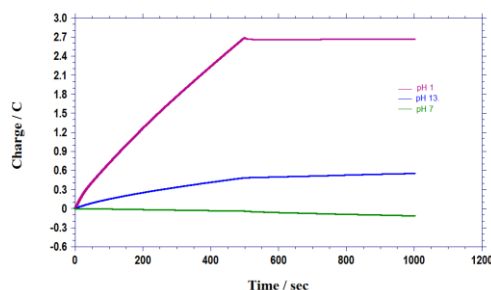


Fig. 10 Chronocolougrams of the composite at pH 1, 7 and 13

Table 3 Charges obtained from chronocoulometric studies

pH	Charge due to double layer capacitance ($\times 10^{-2}$ C)	Surface charge ($\times 10^{-2}$ C)
1	-94.6	-89.887
7	2.186	4.037
13	-13.47	-5.308

4.9 Bulk electrolysis studies

Charge consumed for the electrolysis of the composite is obtained from bulk electrolysis studies. Very less amount of charge is consumed for the electrolysis of this composite at pH 7. This shows that the redox reactions take place much easier in a neutral medium when compared to acidic or basic medium.

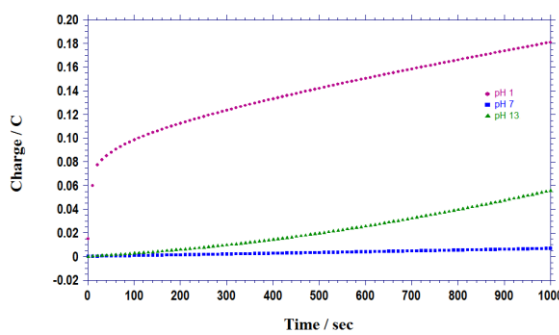


Fig. 11 Bulk electrolysis curves of the composites at pH 1, 7 and 13

Table 4 Charge consumed and current obtained for the composite

pH	Charge consumed ($\times 10^{-2}$ C)	Current (μ A)
1	18.092	73.179
7	0.6820	7.7048
13	5.5773	86.375

5. Conclusions

Polyaniline composite containing benzalazine and cobalt(II) chloride was synthesized

by oxidative polymerization of aniline. FT-IR and UV-Visible studies confirmed the formation of the composite. Cyclic voltammetric studies show that at pH 1 redox reaction took place and at pH 13 only reduction of benzalazine take place. Electrochemical impedance spectroscopy and chronocoulometric studies showed that double layer capacitance for this composite is more at the neutral medium. Less charge is consumed for the electrolysis of this composite at pH 7. So pH 7 is the optimum pH for capacitance studies.

6. Acknowledgements

The authors are thankful to Department of Science and Technology (FAST TRACK & FIST) New Delhi for using electrochemical workstation and UV-Vis spectrometer and UGC New Delhi for FTIR spectroscopy at V.O. Chidambaram College

7. References

- [1] Avanish Pratap Singh, Anoop Kumar S, Amita Chandra, and S. K. Dhawan Conduction mechanism in Polyaniline-flyash composite material for shielding against electromagnetic radiation in X-band & Ku band, *AIP Advances*, 1, 022147, (2011).
- [2] Yakha A Vissurkhanova, Nina M Ivanova and Elena A Soboleva, Electrocatalytic properties of CuCl₂ or FeO doped polyaniline composites in electro hydrogenation of aromatic nitro-compounds, *J Phys Chem Biophys*, 7:2(Suppl), (2017).
- [3] Reza Ansari, Application of Polyaniline and its Composites for Adsorption/Recovery of Chromium (VI) from Aqueous Solutions, *ActaChim. Slov.*, 53, 88–94, (2006).
- [4] Supri Abdul Ghani, Ammar Zakaria, Ali Yeon Md. Shakaff, Mohd. Noor Ahmad and Abu Hassan Abdullah, Enhancing Conductive Polymer Performance Using Eggshell for Ammonia Sensor, *Journal of Physical Science*, 23(2), 73–83, (2012).
- [5] Reza Emamali Sabzi, Kamran Rezapour and NaserSamadi, Polyaniline–multi-wall-carbon nanotube nanocomposites as a dopamine sensor, *J. Serb. Chem. Soc.*, 75 (4) 537–549, (2010).
- [6] Vijayakumar B, Anjana K O and Ranga Rao G, Polyaniline/clay Nanocomposites: Preparation, Characterization and Electrochemical Properties, IOP Conf. Series: *Materials Science and Engineering*, 73, 012112, (2015).
- [7] Mahboobeh Shabandokht, Ehsan Binaeian and Habib-Allah Tayebi, Adsorption of food dye Acid red 18 onto polyaniline-modified rice husk composite: isotherm and kinetic analysis, 1944-3994/1944-3986, (2016).

- [8] Janaki V., Byung-Taek Oh, Shanthi K., Kui-Jae Lee, Ramasamy A.K., Seralathan Kamala-Kannan, Polyaniline/chitosan composite: An eco-friendly polymer for enhanced removal of dyes from aqueous solution, *Synthetic Metals*, 162, 974– 980, (2012).
- [9] Akanksha Mehto, Varsha R Mehto, Jyotsana Chauhan, Singh IB, Pandey RK, Preparation and Characterization of Polyaniline/ZnO Composite Sensor, *Journal of Nanomedicine Research*, 5(1), 1-8, (2017).
- [10] Khosrozadeh A., Wang Q., and Xing M., A high-capacitance solid-state supercapacitor based on polyaniline and ground carbon fibers, Proceedings of the 14th IEEE International Conference on Nanotechnology Toronto, Canada, August 18-21, (2014).
- [11] Rehana Rasool and Kowsar Majid, Synthesis, characterization, thermal and electrical properties of composite of polyaniline with cobaltmonoethanolamine complex, *Bull. Mater. Sci.*, 37(5), 1181–1190, (2014).
- [12] Divya B., Kanagavel D., Karpagavinayagam P. and Vedhi C., Microwave synthesis, electrochemical studies and capacitance of benzalazine, *International Journal of Research in Advent Technology*, 6(9), 2414-2419, (2018).
- [13] Jacek Nizioł, Maciek Sniechowski, Anna Podraza-Guba, Jan Pielichowski, Alternative oxidizers in polyaniline synthesis, *Polym. Bull.*, 66, 761–770, (2011).
- [14] Raju Khan, Puja Khare, Bimala Prasad Baruah, Ajit Kumar Hazarika, Nibaran Chandra Dey, Spectroscopic, Kinetic Studies of Polyaniline-Flyash Composite, *Advances in Chemical Engineering and Science*, 1, 37-44, (2011).
- [15] Kuestan A. Ibrahim, Synthesis and characterization of polyaniline and poly(aniline-co-o-nitroaniline) using vibrational spectroscopy, Arabian journal of Chemistry, *Arabian journal of Chemistry*, 10, s2668-s2674, (2017).
- [16] Yuki Kaitsuka, Noriko Hayashi, Tomoko Shimokawa , Eiji Togawa and Hiromasa Goto, Synthesis of Polyaniline (PANI) in Nano-Reaction Field of Cellulose Nanofiber (CNF), and Carbonization, *Polymers*, 8, 40, (2016).
- [17] Kavitha B., Prabakar K., Siva kumar K., Srinivasu D., Spectroscopic Studies of Nano Size Crystalline Conducting Polyaniline, *IOSR Journal of Applied Chemistry (IOSRJAC)*, 2(1), 16-19, (2012).
- [18] Kakde K. P., synthesis and characterization of polyaniline doped with HCl, H₂SO₄ and PVA as secondary dopant for toxic gas (Ammonia) sensor *Indian Journal of Science and Technology*, 10(20), 1-4, (2017).
- [19] Lela MukmilahYuningsih, Dikdik Mulyadi, Ilham Aripandi, Effect of Various Dopant HCL Concentration on Electrical Conductivity of Pani-Cellulose Composite with Cellulose Isolated from Reed Plant (*Imperata cylindrica* (L.)), *American Journal of Materials Science*, 7(3), 59-63, (2017).
- [20] Mohammad Rezaul Karim, Chul Jae Lee, Mu Sang Lee, Synthesis and Characterization of Conducting Polyaniline-Activated Carbon Nanocomposites, *Journal of Applied Polymer Science*, 103, 1973–1977, (2007).
- [21] Jayasudha S., Priya L., Vasudevan K. T., Preparation and Characterization of Polyaniline/Ag Nanocomposites, *Int.J. ChemTech Res.*, 6(3), 1821-1823, (2014).
- [22] Hichem Zeghoud, Saad Lamouri, Yasmine Mahmoud and Tarik Hadj-Ali, Preparation and characterization of a new polyaniline salt with good conductivity and great solubility in dimethyl sulphoxide, *Journal of Serbian Chemical Society, J. Serb. Chem. Soc.*, 80 (11) 1435–1448, (2015).
- [23] Hichem Zeghoud, Saad Lamouri, Zitouni Safidine and Mohammed Belbachir, Chemical synthesis and characterization of highly soluble conducting polyaniline in mixtures of common solvents, *Journal of the Serbian Chemical Society*, 80(7), 917–931, (2015).
- [24] Giz M.J., de Albuquerque Maranhao S.L., Torresi R.M., AFM morphological study of electropolymerised polyaniline films modified by surfactant and large anions, *Electrochemistry Communications* 2, 377–38, (2000).
- [25] Venancio E.C., Costa C.A.R., Machado S.A.S., Motheo A.J., AFM study of initial stages of polyaniline growth on ITO electrode, *Electrochemistry communications* 3, 229-233, (2001).
- [26] Atanu Roy, Apurba Ray, Priyabrata Sadhukhan, Samik Saha and Sachindranath Das, Morphological behaviour, electronic bond formation and electrochemical performance study of V₂O₅-Polyaniline composite and its application in asymmetric supercapacitor, *Materials Research Bulletin*, 107, 379 – 390, (2018).
- [27] Florian Mansfeld, *An Introduction to Electrochemical Impedance Measurement*, Technical Report No. 26 Part No.: BTR026 Issue: AB:solatron, Analytical, (1999).
- [28] Allen J. Bard, Larry R. Faulkner, *Electrochemical Methods Fundamentals and Applications*, second edition, John Wiley & Sons, (2001).
- [29] Kelly S., Richard, *Analytical Electrochemistry: Basic concepts*.

https://www.asdlib.org/onlineArticles/ecourse_ware/Kelly.../EC_CONCEPTS1.HTM, (2018)

- [30] Adrian W. Bott, Ph.D and William R. Heineman, Ph.D., Bioanalytical Systems, Current Separations, 20(4), 121-126, (2004).